Biochemical and Biophysical Research Communications 385 (2009) 33–37

Contents lists available at ScienceDirect

Biochemical and Biophysical Research Communications

journal homepage: www.elsevier.com/locate/ybbrc

Targeted connexin26 ablation arrests postnatal development of the organ of Corti

Yunfeng Wang [a,c,1], Qing Chang [a,1], Wenxue Tang [a,1], Yu Sun [a], Binfei Zhou [a], Huawei Li [c], Xi Lin [a,b,*]

[a] Department of Otolaryngology, Emory University School of Medicine, 615 Michael Street, Atlanta, GA 30322-3030, USA
[b] Department of Cell Biology, Emory University School of Medicine, 615 Michael Street, Atlanta, GA 30322-3030, USA
[c] Department of Otolaryngology, Eye & ENT Hospital, Fudan University, China

ARTICLE INFO

Article history:
Received 4 May 2009
Available online 9 May 2009

Keywords:
Connexin26 mutation
Cochlear development
Cell degeneration
Spiral ganglion neuron
Hair cells
Mouse models
Genetic deafness
Mechanism of deafness

ABSTRACT

Mutations in the gene coding for connexin26 (Cx26) is the most common cause of human nonsyndromic hereditary deafness. To investigate deafness mechanisms underlying Cx26 null mutations, we generated three independent lines of conditional Cx26 null mice. Cell differentiation and gross cochlear morphology at birth seemed normal. However, postnatal development of the organ of Corti was stalled as the tunnel of Corti and the Nuel's space were never opened. Cell degeneration was first observed in the Claudius cells around P8. Outer hair cell loss was initially observed around P13 at middle turn when inner hair cells were still intact. Massive cell death occurred in the middle turn thereafter and gradually spread to the basal turn, resulting in secondary degeneration of spiral ganglion neurons in the corresponding cochlear locations. These results demonstrated that Cx26 plays essential roles in postnatal maturation and homoeostasis of the organ of Corti before the onset of hearing.

Introduction

Non-sensory cells in the cochlea are connected extensively by gap junctions (GJs) that facilitate intercellular ionic and biochemical coupling. Two protein subunits in the connexin (Cx) family, Cx26 and Cx30, are the prominent members coassembled in most of the cochlear GJs [1,2]. Mutations in the gene coding for Cx26 (*Gjb2*) cause a substantial portion (~20–50%) of human nonsyndromic hereditary deafness cases, resulting in one of the most common human birth defects. In more than 120 reported human *GJB2* mutations linked to prelingual deafness, most of them are loss-of-function mutations that effectively null the utility of Cx26 in the cochlea [3]. Observations made from a previously-published conditional Cx26 (cCx26) null mouse model show that the inner ear developed normally and the sensory hair cells (HCs) degenerated soon after the onset of hearing around P14 [4]. However, phenotypes in conditional gene knockout mice are highly variable depending on the spatial pattern, extent and timing of the deletion of the targeted gene. Therefore, functional studies of cochlear GJs with different types of independent cCx26 null mouse models are essential for drawing any conclusions.

To investigate mechanisms of deafness caused by loss-of-function Cx26 mutations and to circumvent the embryonic lethality in *Gjb2*$^{-/-}$ mice [5], we generated three independent lines of cCx26 null mice. These cCx26 null mouse models were validated by a multidisciplinary approach and confirmed by their profound nonsyndromic congenital deafness. One novel finding agreed by all three types of cCx26 null mice is that the postnatal development of the organ of Corti was stalled as the tunnel of Corti and the Nuel's space were never opened. In addition, we found that the initial site of cell degeneration in the cochlea was in the supporting cells around the outer HCs. Mechanisms explaining why mutations in Cx26 cause deafness are unclear although several plausible theories have been proposed [6]. The developmental arrest that we observed before the occurrence of cell degeneration in the organ of Corti of cCx26 null mice demonstrate a novel developmental function played by Cx26 in the postnatal maturation of the sensory epithelium of the cochlea.

Materials and methods

Generation of three cCx26 null mouse models. Homozygous deletion of *Gjb2* is embryonically lethal due to the defect in glucose transport in the placenta [5]. We therefore deleted *Gjb2* in either

* Corresponding author. Address: Departments of Otolaryngology and Cell Biology, 615 Michael Street, Whitehead Building Room 543, Emory University School of Medicine, Atlanta, GA 30322, USA. Fax: +1 404 727 6256.
E-mail address: xlin2@emory.edu (X. Lin).
[1] These authors contributed equally to this work.

0006-291X/$ - see front matter © 2009 Elsevier Inc. All rights reserved.
doi:10.1016/j.bbrc.2009.05.023

a spatially-specific or time-specific manner. Animal use protocol was approved by the Animal Care and Use Committee of the Emory University. Two of the three cCx26 null mouse models were generated by cross breeding two kinds of genetically-engineered mice:

(1) Mice expressing exogenous Cre recombinase in the cochlea but not in the placenta. The Cre gene is either knocked in at the site of *foxg1* [7] (*foxg1*$^{Cre/+}$ mice) or expressed from a bacterial artificial chromosome (BAC) that contains the Cre coding sequence at the locus of the *pax2* (pax2-cre mice) [8]. Heterozygous *foxg1*$^{cre/+}$ mice were obtained from the Jackson Laboratories (Bar Harbor, ME). Pax2-cre mice were obtained from mutant mouse regional resource centers (http://www.mmrrc.org/). Both *foxg1*$^{Cre/+}$ and pax2-cre mice showed normal hearing (data not shown);
(2) Mice in which the exon2 of the *Gjb2* gene is flanked by the loxP sequence (Cx26$^{loxP/loxP}$ mice). The exon2 of the *Gjb2* contains the entire coding region for the Cx26. Activation of Cre recombinase is expected to totally remove the expression of Cx26. The Cx26$^{loxP/loxP}$ breeding pairs were obtained from the European mouse mutant archive (http://www.emmanet.org/) with the written permission of Dr. Claus Willecke. Previous studies show that the hearing of Cx26$^{loxP/loxP}$ mice is normal [4].

Crossbreeding of the above mice generated foxg1$^{cre/+}$;Cx26$^{loxP/loxP}$ and pax2-Cre;Cx26$^{loxP/loxP}$ mice. They will be called the foxg1-Cre and pax2-Cre cCx26 null mice, respectively. Spatially-specific Cre expression pattern in these mouse models was examined by using the R26R LacZ reporter mice [9] (provided by Dr. Ping Chen, Emory University). Details of the methods for the use of R26R LacZ reporter mice can be found in our previous publications [10].

The third cCx26 null mouse model was generated by removing the *Gjb2* on embryonic day 19 by a single intraperitoneal injection of 4-hydroxytamoxifen (TMX, 1 mg per 10 g body weight, Sigma–Aldrich, St. Louis, MO) to the dams of the Cx26$^{loxP/loxP}$;Rosa26^{CreER} mice. Details for the generation and validation of the time-specific cCx26 null mice were given previously [10]. Genotyping protocols for foxg1$^{cre/+}$;Cx26$^{loxP/loxP}$ [7], pax2-Cre;Cx26$^{loxP/loxP}$ [8], and TMX-inducible [10] cCx26 null mice were given previously.

Methods used for validating mouse models include histological, immunolabeling, Western blotting assays and objective determination of hearing sensitivity. Epoxy resin embedded cochlear sections were prepared by fixing tissues first through cardioperfusion of 4% paraformaldehyde (in PBS). Samples were decalcified in 0.35 M EDTA (pH 7.5, in PBS) for 72 h at 4 °C, followed by gradual dehydration in alcohol of increasing grades, infiltrated, and embedded in epoxy resin with the conventional histological protocols [10]. Cochlear sections (5 μm in thickness, cut with a Microm HM335E microtome, Germany) were stained with toluidine blue.

Polyclonal antibodies against Cx26 and Cx30 were used in immunolabeling and all antibodies used in this study were purchased from Invitrogen Corp (Carlsbad, CA) unless otherwise indicated. These antibodies were fully characterized by Western blots in our published previously [2]. The dilution for the antibody against Cxs was 1:200. The Cx26 and Cx30 labeling was visualized by using a donkey anti-mouse antibody conjugated to rhodamine (1:200 dilution, Jackson ImunoResearch Lab Inc.) and a goat anti-rabbit IgG antibody conjugated to Alexa Fluor 488 (1:500 dilution), respectively. Antibodies against a pillar cell marker P75 [11] (1:200 dilution) and a supporting cell marker Prox1 [12] (1:800 dilution) were obtained from Chemicon (Temecula, CA). Specific markers for HCs, myosin6 or phalloidin, were labeled with antibodies obtained from Proteus bioscience (Ramona, CA) and Sigma–Aldrich Inc. (St. Louis, MO), respectively. Details of the immunolabeling protocols are given previously [13]. Processed samples were examined using a conventional fluorescent microscope (Zeiss Axiovert 135TV, Carl Zeiss).

For Western blot we isolated total proteins separately from the organ of Corti (including the spiral limbus region), stria vascularis and spiral ligament with the RIPA lysis buffer by following the manufacturer's instructions (Upstate Biotechnology Cell Signaling System, Lake Placid, NY). Protein concentrations were measured by using a bicinchoninic acid protein assay kit (Pierce, Rockford, IL). Equal amount of protein (5 μg) was loaded in each lane and proteins were separated by electrophoresis on a 12% sodium dodecyl sulfate polyacrylamide gel. After transferring to nitrocellulose membrane, bands of Cxs were detected by using the same Cx26 (0.25 μg/ml) and Cx30 (0.5 μg/ml) we used in immunolabeling. Secondary antibodies used in the Western blots were goat anti-rabbit Cx26 conjugated with HRP (Bio-Rad Laboratories Inc., Hercules, CA). Protein bands on the blots were visualized by enhanced chemiluminescence (Super-Signal, Pierce, Rockford, IL) exposed on X-ray films (Hyper Film, Amersham Biosciences, Piscataway, NJ). Cx proteins were quantified on digitized images by normalizing to the WT controls (AlphaEase software, version4.1, Alpha Innotech Corp., Sanleandro, CA). Auditory brainstem responses (ABRs) measure sound-evoked far-field potentials, which are widely used to determine hearing thresholds objectively. Details of the testing methods for the ABRs are given in our previously-published papers [13].

Results

Validation of TMX-inducible cCx26 null mice was described in our published paper [10]. Here we describe the data validating the two new cCx26 null mouse models obtained by deleting the *Gjb2* in a spatially-specific manner. Patterns of Cre recombinase expression in the cochlea of foxg1-Cre (Fig. 1A) and pax2-Cre (Fig. 1B) cCx26 null mice were examined by utilizing the R26R LacZ reporter mice [9], which demonstrated strong Cre activities in the organ of Corti, spiral limbus and the spiral ganglia. In contrast, the Cre activation in the stria vascularis and lateral wall was weak (Fig. 1A and B). Consistent with this pattern, Western blot quantification of Cx26 protein levels revealed that the largest reduction was in the organ of Corti and spiral limbus (Fig. 1C, panel on the top). Comparing to the wild type (WT) controls, the Cx26 protein in the organ of Corti of foxg1-Cre and pax2-Cre cCx26 null mice was 11.2 ± 3.3% and 9.1 ± 4.2%, respectively ($n = 4$). In contrast, changes of Cx26 protein in the spiral ligament and stria vascularis were both statistically insignificant ($p > 0.05$) (Fig. 1C, panels in the middle and bottom). This pattern of Cx26 reduction in the cochlea of cCx26 null mice was supported by immunolabeling data (Fig. 1E). Since Cx26 and Cx30 are co-expressed in almost all cochlear GJs [1,2] , co-immunolabeling with an antibody against Cx30 was used as a control. Cx30 immunoreactivities were identified in the cell membrane of supporting cells in the organ of Corti (Fig. 1E, top left panel) and spiral limbus (Fig. 1E, top right panel), presumably forming homomeric GJs in the cochlea of cCx26 null mice. In contrast to the uninterrupted network of GJs suggested by Cx30 immunoreactivity (Fig. 1E, top panels), the pattern of Cx26 showed absence of Cx26 in most of the cells (red fluorescence in Fig. 1E, bottom two panels). The incomplete deletion of *Gjb2* in some cells is demonstrated by arrows in Fig. 1E showing examples of some cells in the spiral limbus where Cx26 was still detected.

The foxg1-Cre ($n = 60$) and pax2-Cre ($n = 48$) cCx26 null mice have normal body weight and are fertile with normal litter size. These mouse models for human Cx26 mutations were confirmed further by the non-syndromic deafness displayed in all the mutant mice (Fig. 1D). ABRs measured across a frequency range of 4–

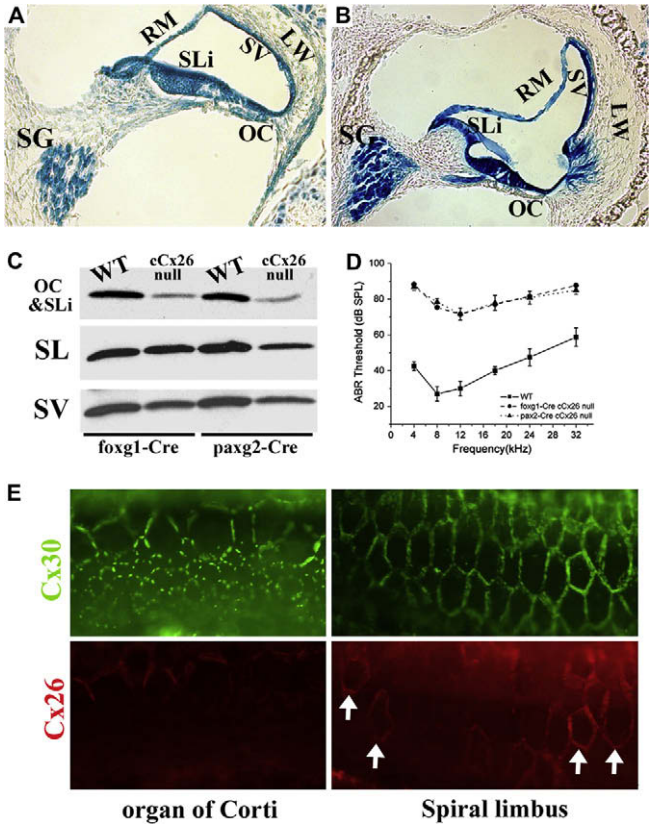

Fig. 1. Validation of cCx26 null mouse models by various methods. Cre activities in the cochlea driven by the *foxg1* (A) and *pax2* (B) were reported by the LacZ staining in R26R reporter mice. *Abbreviations:* SLi, spiral limbus; RM, Reissner's membrane; SV, stria vascularis; OC, organ of Corti; SG, spiral ganglia. (C) The Western blots of Cx26 from the organ of Corti and spiral limbus (top), spiral ligament (SL, middle), and stria vascularis (bottom) of WT and the two cCx26 null mice. (D) gives the hearing thresholds (*y*-axis) as a function of frequency (*x*-axis) measured by ABRs. Legends for different mouse groups are given in the panel. (E) The co-immunolabeling results of Cx30 and Cx26 obtained from organ of Corti and the spiral limbus.

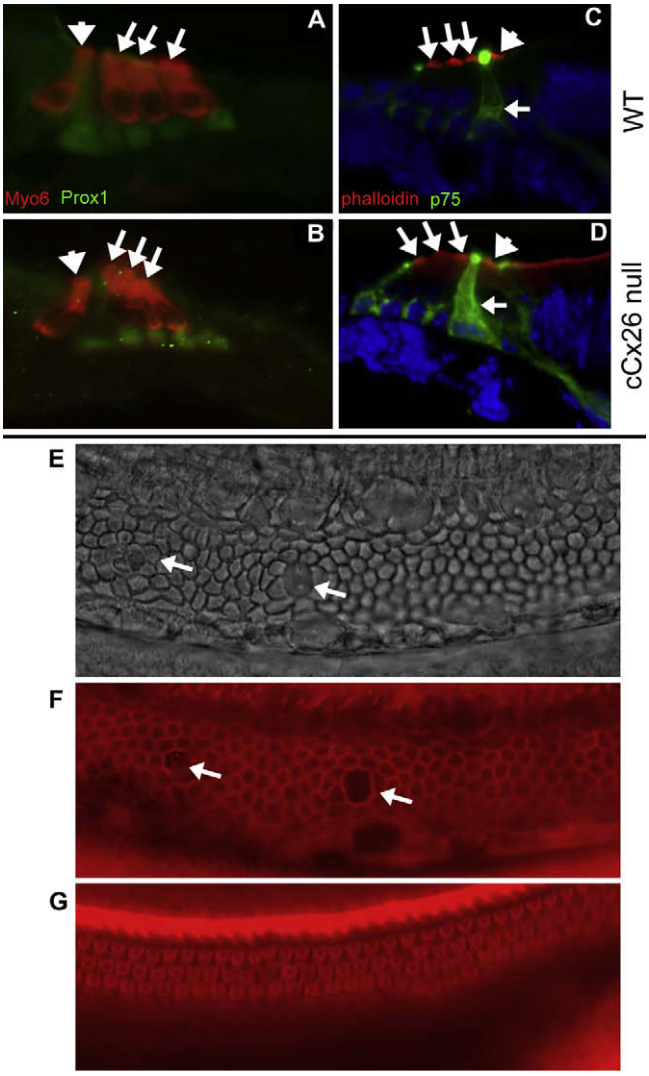

Fig. 2. Cell differentiation and degeneration in the organ of Corti. (A–D) Cellular structures of the organ of Corti at P0 were compared between WT and cCx26 null mice. Hair cell and supporting cell specific markers were immunolabeled. (E–G) A P8 old whole-mount cochlear sample was viewed with either conventional optics (E) or fluorescent labeling of phalloidin to visualize the cell borders. The phalloidin labeling also shows the stereocilia of HCs (G) for this segment of the cochlea.

32 kHz showed that hearing thresholds in these mutant mice were elevated by about 40–50 dB (Fig. 1D) comparing to their littermate-control mice that didn't carry the Cre gene ($n = 17$). In summary, four independent lines of evidence presented above support that we have obtained valid mouse models for studying deafness caused by conditional Cx26 null expression in the cochlea.

Using the cCx26 null mice, we first examined whether prenatal cell differentiation in the organ of Corti is completed. Immunolabeling with specific hair cell markers showed typical structure of one row of inner HCs (arrowhead in Fig. 2A–D), three rows of outer HCs (small arrows in Fig. 2A–D) in both WT (Fig. 2A and C) and mutant (Fig. 2B and D) mice. Patterns of supporting cell arrangements around the HCs were examined with antibodies against p75 (horizontal arrows in Fig. 2C and D) and Prox1 (green fluorescence in Fig. 2A and B). Results obtained from WT (Fig. 2A and C) and cCx26 null mice (Fig. 2B and D) were indistinguishable. These immunolabeling results suggested that hair cell and supporting cell differentiation in the organ of Corti of cCx26 null mice was not affected.

Gross cochlear morphology in cCx26 null mice appeared to be normal, with no obvious collapse or expansion of the Reissner's membrane. No apparent defects were observed in the development of the tectorial membrane, inner spiral tunnel and the stria vascularis (Fig. 1, Fig. 3 and Fig. 4G, H). By observing cochlear samples obtained at a series of postnatal development stages, we found that the initial degeneration in the organ of Corti of cCx26 null mice was in the Claudius cells around P8 (arrows in Fig. 2E and F). In contrast, the HCs showed normal orientation and arrangement of their stereocilia at the same developmental stage (Fig. 2G). Fig. 3 compares morphology of the organ of Corti of WT and three cCx26 null mouse models obtained at a series of developmental stages. All three mouse models yielded consistent spatial and temporal morphological changes in the organ of Corti. Inner and outer HCs are present in both WT (Fig. 3, arrowheads in all the panels) and cCx26 null (Fig. 3B–D, small arrows) mice at birth. General structures of the organ of Corti were indistinguishable between WT and mutant mice before P9. A major difference emerged around P9 when the tunnel of Corti and the Nuel's space in the middle cochlear turn opened in the WT (Fig. 3E, panels in the first column) but not in any of the cCx26 null mice (Fig. 3F–H, upward white arrows). The development of tectorial membrane (Fig. 3E–L) and the inner spiral tunnel (Fig. 3E–L) appeared to be normal in the mutant mice. Dramatic cell death occurred around P13 in the outer HCs and the surrounding supporting cells (big black arrowheads in Fig. 3J–L). Consistent with the results obtained from the whole-

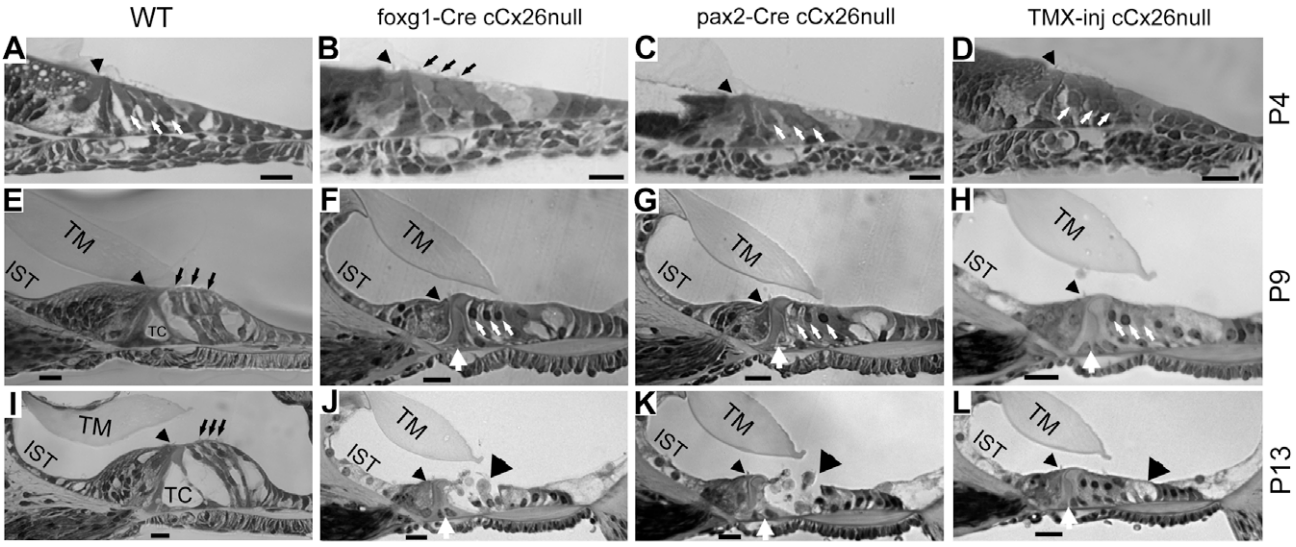

Fig. 3. Comparison of the morphology of the organ of Corti at the middle turn in WT (panels in the first column) and three cCx26 null mouse models at P4 (top panels), P9 (middle panels) and P13 (bottom panels). *Abbreviations:* TC, tunnel of Corti; TM, tectorial membrane; IST, inner spiral tunnel. Scales represent approximately 100 μm.

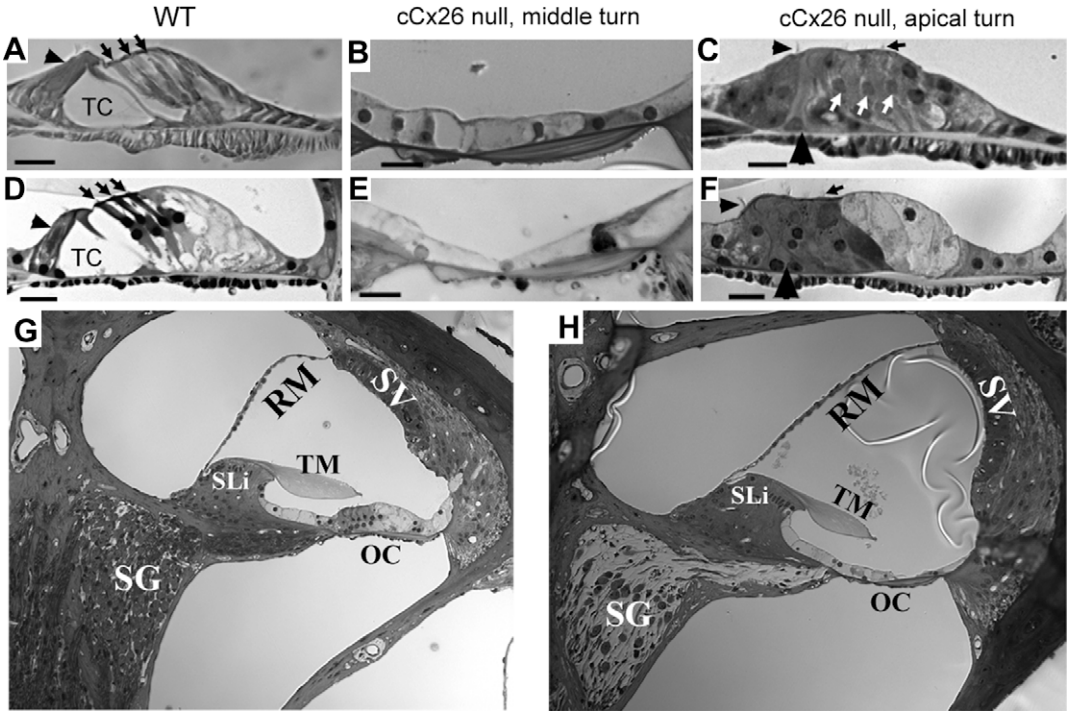

Fig. 4. Comparison of the morphology of the organ of Corti in WT (A, D) and cCx26 null mice at middle (B, E) and apical (C, F) turns. Cochlear samples obtained at P16 (A–C) and P30 (D–F) are given. Whole cochlear sections of adult mice (P30) at apical (G) and middle (H) turns are shown to demonstrate the secondary degeneration of spiral ganglion neurons at the middle turn (H). Abbreviations used are the same as previous figures. Scales represent approximately 100 μm.

mount cochlear preparations (Fig. 2E and F), Claudius cells in cochlear sections also show signs of degeneration before the outer HCs die (big arrowhead in Fig. 3L). The inner HCs, in contrast, were intact judged by the presence of stereocilia (pointed by small arrowheads in Fig. 3J–L) at the time when outer HCs were disintegrated (big arrowheads in Fig. 3J and K). The tunnel of Corti was still closed at P13. Presence of intact pillar cells was supported by the two nuclei (upward white arrows in Fig. 3J–L).

Only a layer of non-specific epithelial cells were left in the middle turn organ of Corti around P16 (Fig. 4B). By P30, cells in a large segment of the middle turn in the organ of Corti were dead (Fig. 4E). Cell degeneration progressed gradually from the middle turn to the basal turn. A dramatic contrast is that all types of cells in the apical turn organ of Corti survived for at least six months (longest period we have observed so far). Both the nuclei (white arrows in Fig. 4C) and stereocilia (horizontal arrowheads in Fig. 4C and F) of inner and outer HCs are present. The tunnel of Corti and the Nuel's space (TC in Fig. 4A and D), however, were never opened in the mutant mice (upward arrowheads in Fig. 4C and F). The spiral ganglion neurons were also degenerated in the corresponding locations. While neurons in the apical turn were essentially intact (Fig. 4G), most of them in the middle and basal turns disappeared by P30 in the Rosenthal's canal in the cCx26 null mice (Fig. 4H).

Discussion

In altricial animals (e.g., mouse, rat), the hearing organ is born immature and the organ of Corti continues to develop postnatally to reach the mature cellular structure. The auditory sensory organ is not ready for sound transduction until P12 in mice [14]. One of the landmark morphological development just before the onset of hearing is the opening of the tunnel of Corti and formation of the Nuel's spaces. Specific loss or development delay of these structures in the organ of Corti is known to cause profound hearing loss [15]. Mechanisms of deafness caused by loss-of-function Cx26 mutations are unknown. Currently-prevailing hypotheses, however, focus on dysfunctions brought on by the loss of GJ-mediated functions after onset of hearing [6]. The most important finding of this study is that Cx26 plays essential roles in postnatal maturation of the organ of Corti before the onset of hearing. Although the first cCx26 null mouse model [4] showed normal inner ear development until P14, data obtained from all three independent cCx26 mouse models here and a recently-published dominant negative (R75W point mutation) *Gjb2* transgenic mouse model [16] agree that postnatal development of the organ of Corti was arrested before the occurrence of cell death in the organ of Corti. Therefore, a novel developmental role played by Cx26 in the maturation of the cochlear sensory epithelium is supported by four independent Cx26 mutant mouse models.

Dysfunction of GJ-mediated K^+ recycling in the cochlea has been the most frequently-cited hypothesis [6]. Endolymphatic K^+ enters hair cells through mechanotransduction channels during sound-evoked activities. The K^+ recycling theory proposes that the K^+ ions accumulated around the base of hair cells are quickly absorbed by cochlear supporting cells through GJ-mediated intercellular transfer and recycled back to the endolymph [6]. Many aspects of our findings are inconsistent with the predictions of the K^+ recycling theory. Inner HCs are the true transducers that connect to about 95% of the auditory afferent fibers. They should be the most vulnerable to the damage caused by extracellular K^+ accumulation. However, we found that the initial site of degeneration in the organ of Corti of cCx26 null mice was in the Claudius cells (Fig. 2E–F). Inner HCs are clearly present when outer HCs are already disintegrated (Fig. 3J and K). Major events in the K^+ recycling theory should happen after the onset of hearing since they depend on sound-driven activities. Therefore effects of Cx26 null mutation on the development of the organ of Corti is not predicted by the K^+ recycling theory. Immunolabeling data obtained from the cochlea of cCx26 null mice (Fig. 1E) [4] support the existence of remaining homomeric GJs in the cochlea. Additionally, Cx26 point mutations specifically blocking biochemical coupling (e.g., V84L, V95 M, and A88S) are sufficient to cause deafness in humans [17,18]. Disruption on the biochemical coupling provided by GJs in the cochlea is suggested as a major deafness mechanism in the Cx30 null mutant mice [19]. Similarly, significantly-reduced supply of growth factors and nutrient molecules may hinder the postnatal maturation of the organ of Corti in the cCx26 null mice at a postnatal period well before the K^+ recycling is functionally required in the cochlea. This appears to be a testable hypothesis that worth pursuing by future studies.

Acknowledgments

This study was supported by grants to XL from NIDCD (RO1-DC006483 and R21-DC008353) and from National Natural Science Foundation of China (30728029), and also by grant supports to WT from NIDCD (R21 DC008672) and the Deafness Research Foundation. Yunfeng Wang and Yu Sun received support from China Scholarship Council, Grant #2008610021 and 200710187, respectively.

References

[1] A. Forge, D. Becker, S. Casalotti, J. Edwards, N. Marziano, G. Nevill, Gap junctions in the inner ear: comparison of distribution patterns in different vertebrates and assessment of connexin composition in mammals, J. Comp. Neurol. 467 (2003) 207–231.
[2] S. Ahmad, S. Chen, J. Sun, X. Lin, Connexins 26 and 30 are co-assembled to form gap junctions in the cochlea of mice, Biochem. Biophys. Res. Commun. 307 (2003) 362–368.
[3] E. Hoang Dinh, S. Ahmad, Q. Chang, W. Tang, B. Stong, X. Lin, Diverse deafness mechanisms of connexin mutations revealed by studies using in vitro approaches and mouse models, Brain Res. (2009).
[4] M. Cohen-Salmon, T. Ott, V. Michel, J.P. Hardelin, I. Perfettini, M. Eybalin, T. Wu, D.C. Marcus, P. Wangemann, K. Willecke, C. Petit, Targeted ablation of connexin26 in the inner ear epithelial gap junction network causes hearing impairment and cell death, Curr. Biol. 12 (2002) 1106–1111.
[5] H.D. Gabriel, D. Jung, C. Butzler, A. Temme, O. Traub, E. Winterhager, K. Willecke, Transplacental uptake of glucose is decreased in embryonic lethal connexin26-deficient mice, J. Cell Biol. 140 (1998) 1453–1461.
[6] B.A. Schulte, J.C. Adams, Distribution of immunoreactive Na^+, K^+-ATPase in gerbil cochlea, J. Histochem. Cytochem. 37 (1989) 127–134.
[7] U. Pirvola, J. Ylikoski, R. Trokovic, J.M. Hebert, S.K. McConnell, J. Partanen, FGFR1 is required for the development of the auditory sensory epithelium, Neuron 35 (2002) 671–680.
[8] T. Ohyama, A.K. Groves, Generation of Pax2-Cre mice by modification of a Pax2 bacterial artificial chromosome, Genesis 38 (2004) 195–199.
[9] P. Soriano, Generalized lacZ expression with the ROSA26 Cre reporter strain, Nat. Genet. 21 (1999) 70–71.
[10] Y. Sun, W. Tang, Q. Chang, Y.F. Wang, Y.Y. Kong, X. Lin, Connexin30 null and conditional connexin26 null mice display distinct pattern and time course of cellular degeneration in the cochlea, J. Comp. Neurol., in press.
[11] G. Gestwa, B. Wiechers, U. Zimmermann, M. Praetorius, K. Rohbock, I. Kopschall, H.P. Zenner, M. Knipper, Differential expression of trkB.T1 and trkB.T2, truncated trkC, and p75(NGFR) in the cochlea prior to hearing function, J. Comp. Neurol. 414 (1999) 33–49.
[12] C. Jones, V.C. Roper, I. Foucher, D. Qian, B. Banizs, C. Petit, B.K. Yoder, P. Chen, Ciliary proteins link basal body polarization to planar cell polarity regulation, Nat. Genet. 40 (2008) 69–77.
[13] S. Ahmad, W. Tang, Q. Chang, Y. Qu, J. Hibshman, Y. Li, G. Sohl, K. Willecke, P. Chen, X. Lin, Restoration of connexin26 protein level in the cochlea completely rescues hearing in a mouse model of human connexin30-linked deafness, Proc. Natl. Acad. Sci. USA 104 (2007) 1337–1341.
[14] R. Pujol, M. Lavigne-Rebillard, M. Lenoir, Development of sensory and neural structures in the mammalian cochlea, in: E.W. Rubel, A.N. Popper, R.R. Fay (Eds.), Development of the Auditory System, Springer, New York, 1998, pp. 146–192.
[15] D. Forrest, T.A. Reh, A. Rusch, Neurodevelopmental control by thyroid hormone receptors, Curr. Opin. Neurobiol. 12 (2002) 49–56.
[16] A. Inoshita, T. Iizuka, H.O. Okamura, A. Minekawa, K. Kojima, M. Furukawa, T. Kusunoki, K. Ikeda, Postnatal development of the organ of Corti in dominant-negative Gjb2 transgenic mice, Neuroscience 156 (2008) 1039–1047.
[17] Y. Zhang, W. Tang, S. Ahmad, J.A. Sipp, P. Chen, X. Lin, Gap junction-mediated intercellular biochemical coupling in cochlear supporting cells is required for normal cochlear functions, Proc. Natl. Acad. Sci. USA 102 (2005) 15201–15206.
[18] M. Beltramello, V. Piazza, F.F. Bukauskas, T. Pozzan, F. Mammano, Impaired permeability to Ins(1, 4, 5)P3 in a mutant connexin underlies recessive hereditary deafness, Nat. Cell Biol. 7 (2005) 63–69.
[19] Q. Chang, W. Tang, S. Ahmad, B. Zhou, X. Lin, Gap junction mediated intercellular metabolite transfer in the cochlea is compromised in connexin30 null mice, PLoS ONE 3 (2008) e4088.